ICCE 2018
36TH INTERNATIONAL CONFERENCE ON COASTAL ENGINEERING 2018
Baltimore, Maryland | July 30 – August 3, 2018
The State of the Art and Science of Coastal Engineering

NUMERICAL MODELING OF WAVE INTERACTION WITH A NON-CONVENTIONAL BREAKWATER FOR WAVE ENERGY ONVERSION

Enrico Di Lauro[1], Maria Maza[2], **Javier L. Lara**[2], Inigo J. Losada[2], Diego Vicinanza[1]

[1]Università della Campania "Luigi Vanvitelli

[2]Environmental Hydraulics Institute, IH Cantabria, Universidad de Cantabria

OUTLINE

1. INTRODUCTION
2. DESCRIPTION OF THE NUMERICAL MODEL
3. DESCRIPTION OF THE EXPERIMENTAL SETUP
4. NUMERICAL MODEL SETUP
5. RESULTS
6. FUTURE APPLICATIONS
7. CONCLUSIONS

OUTLINE

1. INTRODUCTION
2. DESCRIPTION OF THE NUMERICAL MODEL
3. DESCRIPTION OF THE EXPERIMENTAL SETUP
4. NUMERICAL MODEL SETUP
5. RESULTS
6. FUTURE APPLICATIONS
7. CONCLUSIONS

1. INTRODUCTION

Innovative Breakwater = Breakwater integrated with Wave Energy Converters (WECs)

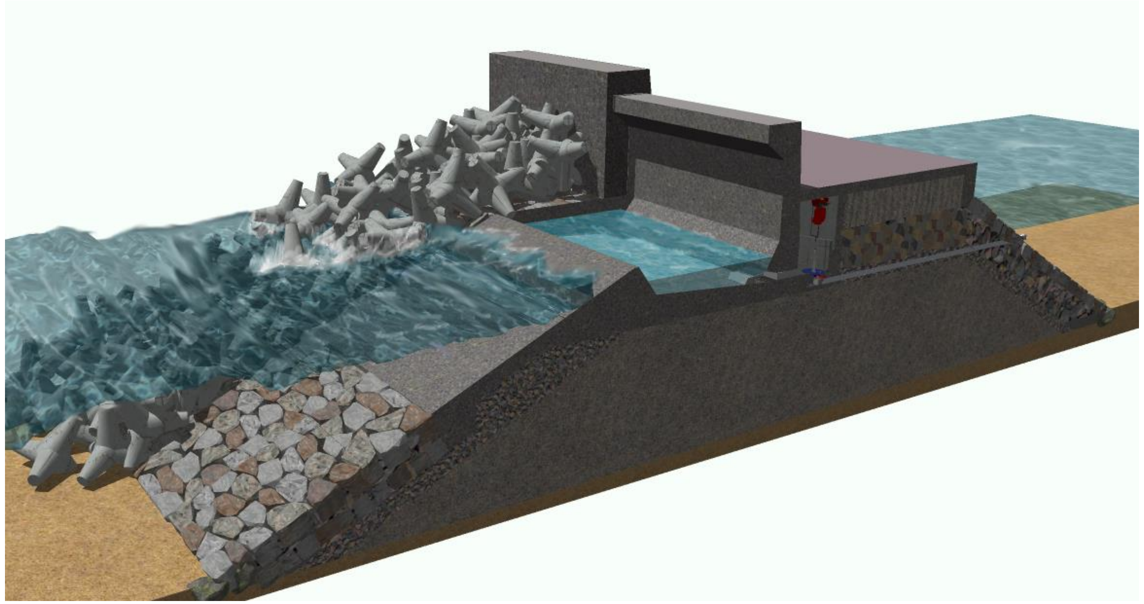

The primary function of these "*non-conventional breakwater*" remains the **harbour/coastal protection…**
with the important co-benefit of the **energy production**.

~~DISSIPATE WAVE ENERGY~~ → CAPTURE THE WAVE ENERGY → Provide useful energy [electricity]

Cost reduction:
breakwater would be built regardless of the inclusion of a WEC
(sharing-cost due to integration)

High reliability:
performances and global stability evaluated with well-established methodologies used in coastal engineering for traditional breakwaters

OBREC DEVICE AT THE PORT OF NAPLES (ITALY)

1. INTRODUCTION

Overtopping Wave Energy Converter (OTD) **embedded** into breakwater

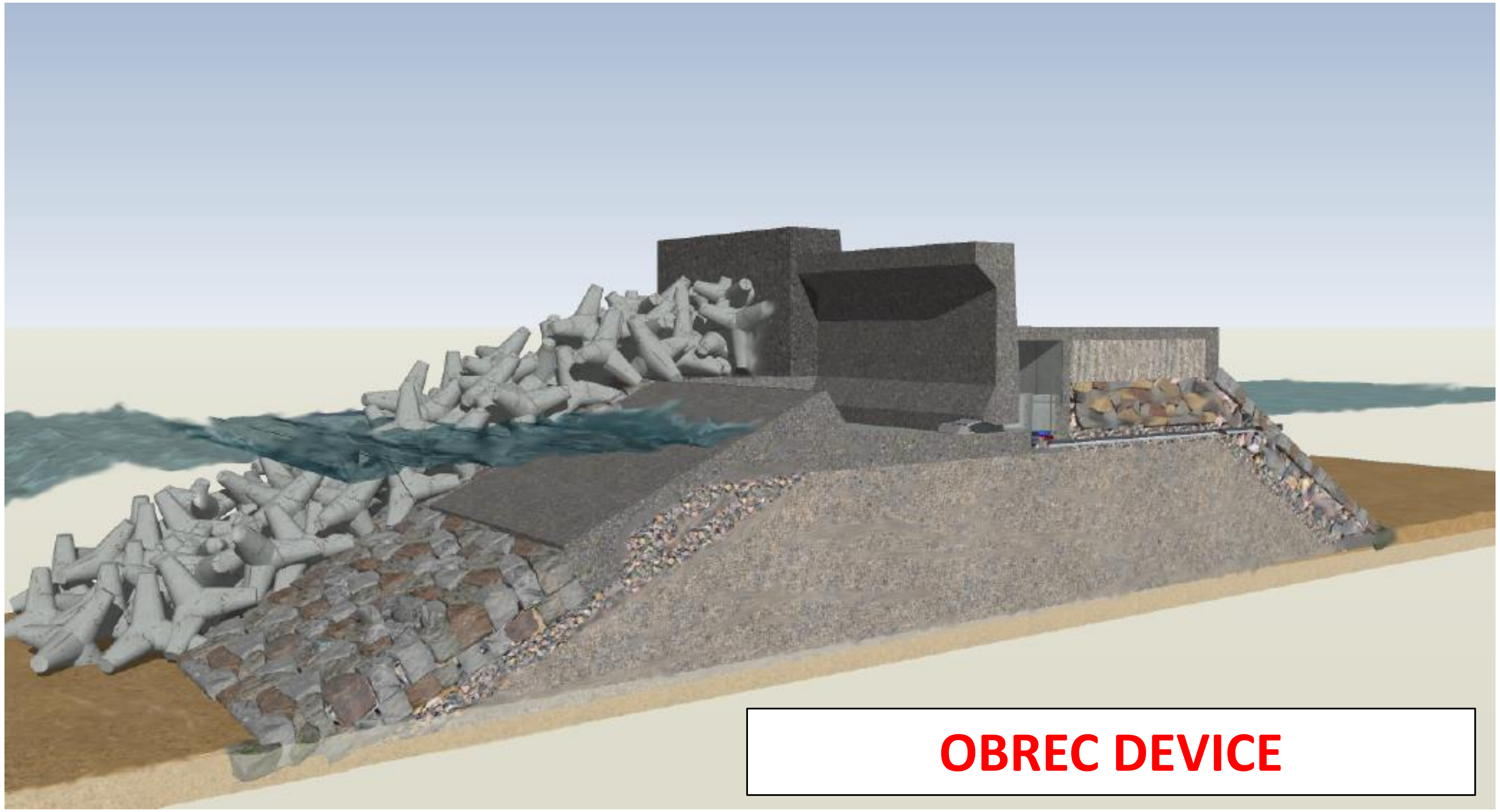
OBREC DEVICE

The device consists of a rubble mound breakwater with a front reservoir designed to capture the **wave overtopping** in order to convert wave energy into potential energy.

Water stored in the reservoir produces energy by flowing through **low-head hydraulic turbines**, exploiting the difference in water level between the reservoir and the main sea water level.

OUTLINE

1. INTRODUCTION
2. DESCRIPTION OF THE NUMERICAL MODEL
3. DESCRIPTION OF THE EXPERIMENTAL SETUP
4. NUMERICAL MODEL SETUP
5. RESULTS
6. FUTURE APPLICATIONS
7. CONCLUSIONS

2. DESCRIPTION OF THE NUMERICAL MODEL

IH-2VOF solves the Volume-Averaged Reynolds-Averaged Navier–Stokes (**VARANS**) Equations, based on the decomposition of the instantaneous velocity, *v*, and pressure fields, *p*, into mean and turbulent components.

The VARANS equations, derived by the integration of the RANS equations over a control volume, are coupled with the **volume-averaged k-ϵ turbulence closure model** (*Hsu et al., 2002*).

The free surface movement is tracked by the ***VOF method***.

$$\frac{\partial\langle\bar{u}_i\rangle}{\partial x_i}=0$$

$$\begin{aligned}(1+c_m)\frac{\partial}{\partial t}\left[\frac{\rho\langle\bar{u}_i\rangle}{n}\right]+\frac{1}{n}\frac{\partial}{\partial x_j}\left[\frac{\rho\langle\bar{u}_j\rangle\langle\bar{u}_i\rangle}{n}\right]+\frac{1}{n}\frac{\partial}{\partial x_j}\left[\rho\langle\overline{u_i'u_j'}\rangle\right]\\ =-\frac{\partial\langle\bar{p}\rangle^f}{\partial x_i}+\rho g_i+\frac{1}{n}\frac{\partial}{\partial x_j}\left[\mu\frac{\partial\langle\bar{u}_i\rangle}{\partial x_j}\right]\\ -\frac{1}{n}\left[\alpha\frac{(1-n)^2}{n^2}\frac{\mu}{{D_{50}}^2}\langle\bar{u}_i\rangle+\beta\left(1+\frac{7.5}{KC}\right)\frac{1-n}{n^2}\frac{\rho}{D_{50}}\sqrt{\langle\bar{u}_j\rangle\langle\bar{u}_j\rangle}\langle\bar{u}_i\rangle\right]\end{aligned}$$

IH 2VOF

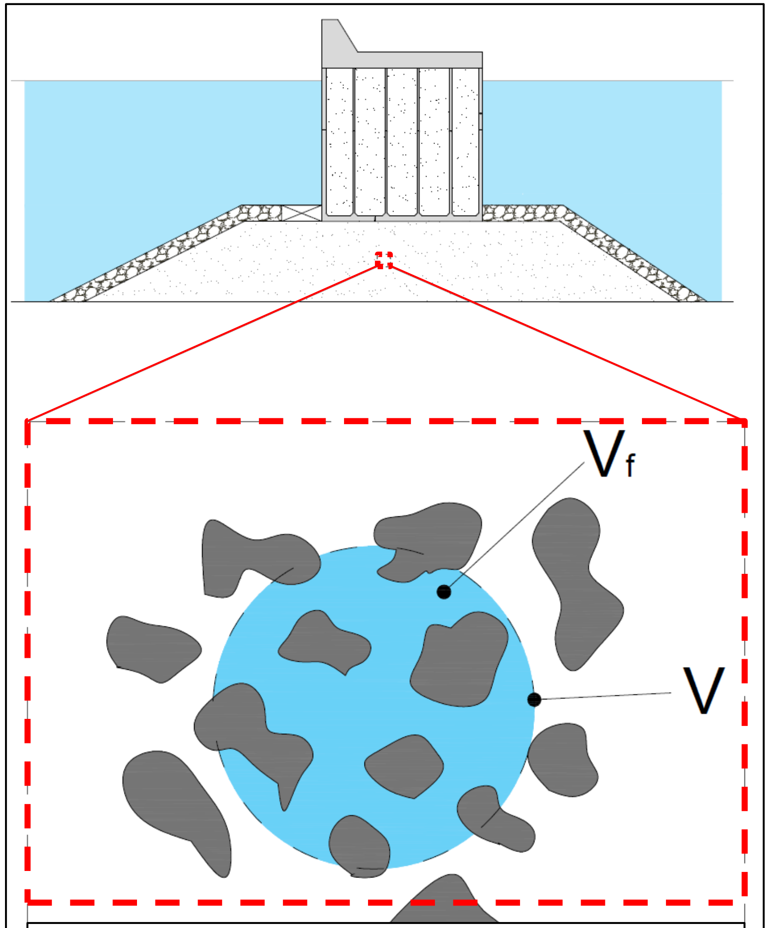

Volume averaging process

$$\langle a\rangle^f=\frac{1}{V_f}\int_{V_f}a\,dV\qquad\langle a\rangle=\frac{1}{V}\int_{V_f}a\,dV$$

$$\Rightarrow\langle a\rangle=n_e\langle a\rangle^f\qquad n_e=\frac{V_f}{V},\ \text{(Porosity)}$$

2. DESCRIPTION OF THE NUMERICAL MODEL

IH-2VOF solves the Volume-Averaged Reynolds-Averaged Navier–Stokes **(VARANS)** Equations, based on the decomposition of the instantaneous velocity, *v*, and pressure fields, *p*, into mean and turbulent components.

The VARANS equations, derived by the integration of the RANS equations over a control volume, are coupled with the **volume-averaged k-ϵ turbulence closure model** (*Hsu et al., 2002*).

The free surface movement is tracked by the ***VOF method***.

Henry Darcy

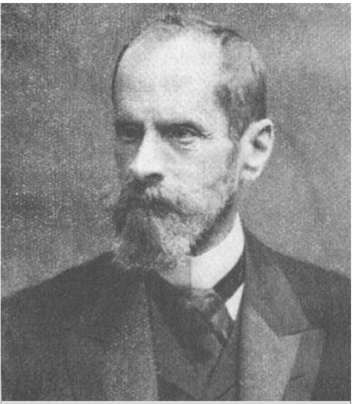

Philipp Forchheimer

The interfacial forces between the fluid and solid are **modelled** by means the **Darcy-Forchheimer relation** which includes the linear and non-linear drag forces here expressed according to *van Gent (1995)*.

The empirical coefficients **α and β evaluated by comparing experimental data and numerical results.**

$$\frac{\partial \langle \overline{u_i} \rangle}{\partial x_i} = 0$$

$$\begin{aligned} &(1+c_m)\frac{\partial}{\partial t}\left[\frac{\rho\langle\overline{u_i}\rangle}{n}\right] + \frac{1}{n}\frac{\partial}{\partial x_j}\left[\frac{\rho\langle\overline{u_j}\rangle\langle\overline{u_i}\rangle}{n}\right] + \frac{1}{n}\frac{\partial}{\partial x_j}\left[\rho\langle\overline{u_i' u_j'}\rangle\right] \\ &= -\frac{\partial\langle\overline{p}\rangle^f}{\partial x_i} + \rho g_i + \frac{1}{n}\frac{\partial}{\partial x_j}\left[\mu\frac{\partial\langle\overline{u_i}\rangle}{\partial x_j}\right] \\ &\boxed{-\frac{1}{n}\left[\alpha\frac{(1-n)^2}{n^2}\frac{\mu}{{D_{50}}^2}\langle\overline{u_i}\rangle + \beta\left(1+\frac{7.5}{KC}\right)\frac{1-n}{n^2}\frac{\rho}{D_{50}}\sqrt{\langle\overline{u_j}\rangle\langle\overline{u_j}\rangle}\langle\overline{u_i}\rangle\right]} \end{aligned}$$

$$KC = \frac{T_0 \cdot u_M}{D_{50} \cdot n}$$ *Keulegan-Carpenter number*

$$c_m = c\,\frac{1-n}{n}$$ *Added mass coeff. (c=0.34)*

OUTLINE

1. INTRODUCTION
2. DESCRIPTION OF THE NUMERICAL MODEL
3. **DESCRIPTION OF THE EXPERIMENTAL SETUP**
4. NUMERICAL MODEL SETUP
5. RESULTS
6. FUTURE APPLICATIONS
7. CONCLUSIONS

3. DESCRIPTION OF THE EXPERIMENTAL SETUP

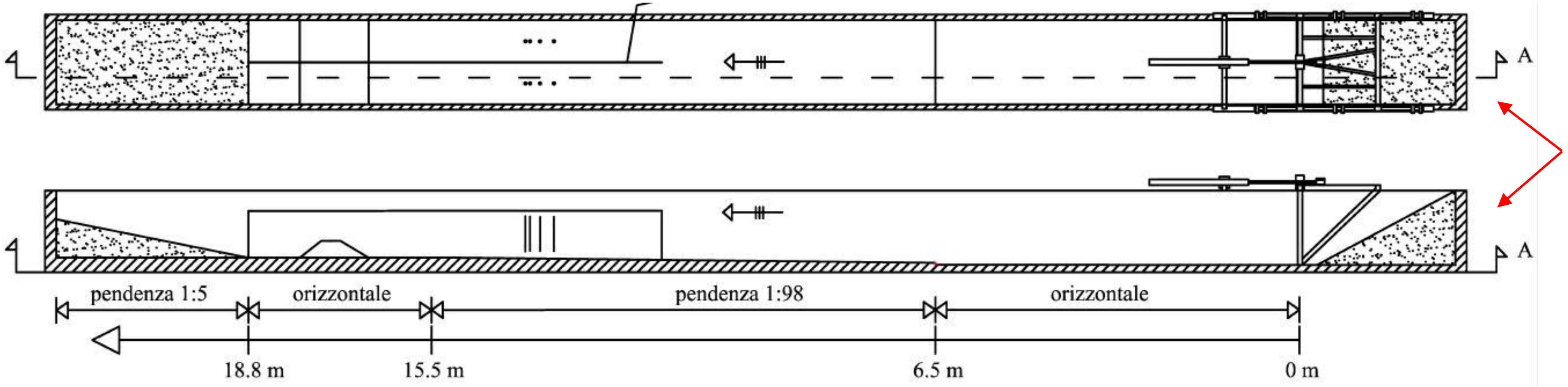

Piston-type wavemaker with Active Wave Absorption

Wave flume:
- 25 m long
- 1.50 m wide
- 1.2 m deep

(Scale 1:30)

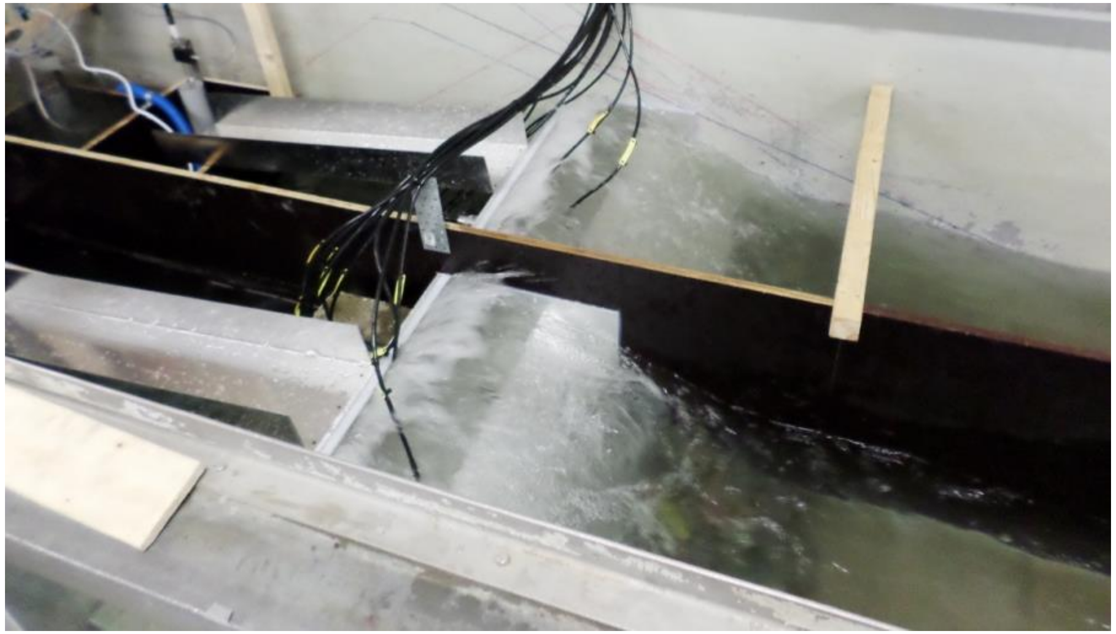

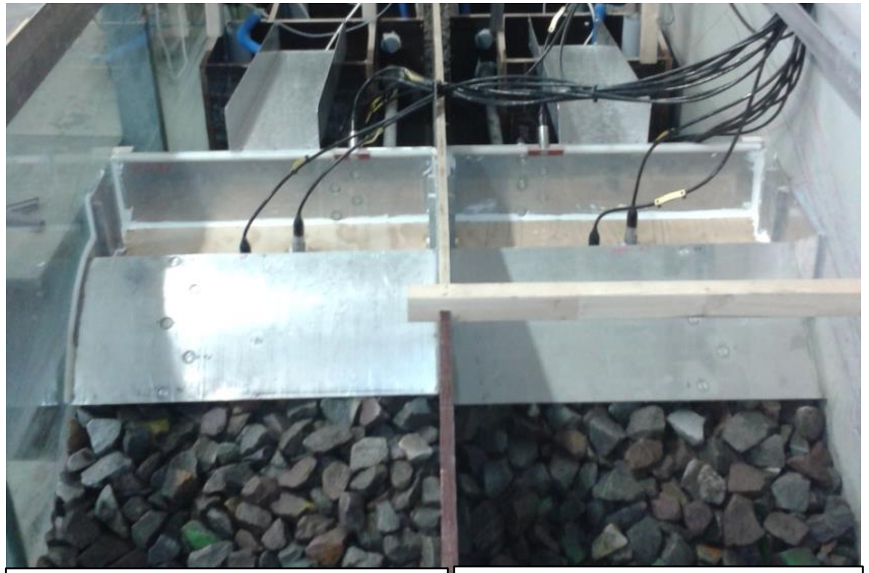

Curved Configuration *Flat Configuration*

Contestabile, P., Iuppa, C., **Di Lauro, E.**, Cavallaro, L., Lykke Andersen, T., Vicinanza, D., (2017). Wave loadings acting on innovative rubble mound breakwater for overtopping wave energy conversion, Coastal Engineering, 60-74.

3. DESCRIPTION OF THE EXPERIMENTAL SETUP

8 **resistive wave gauges**, displaced in the wave flume in two parallel arrays:

- Measure the free surface time series;
- Separate incident and reflected waves.

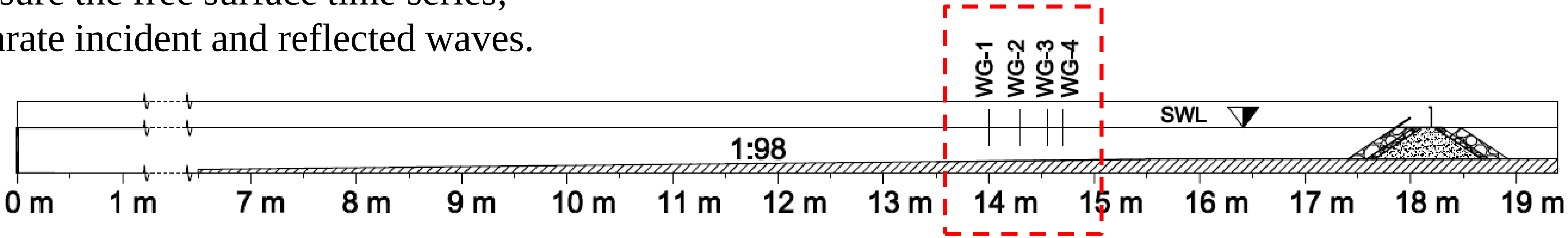

Numerical model has been validated using only the **flat device configuration**.

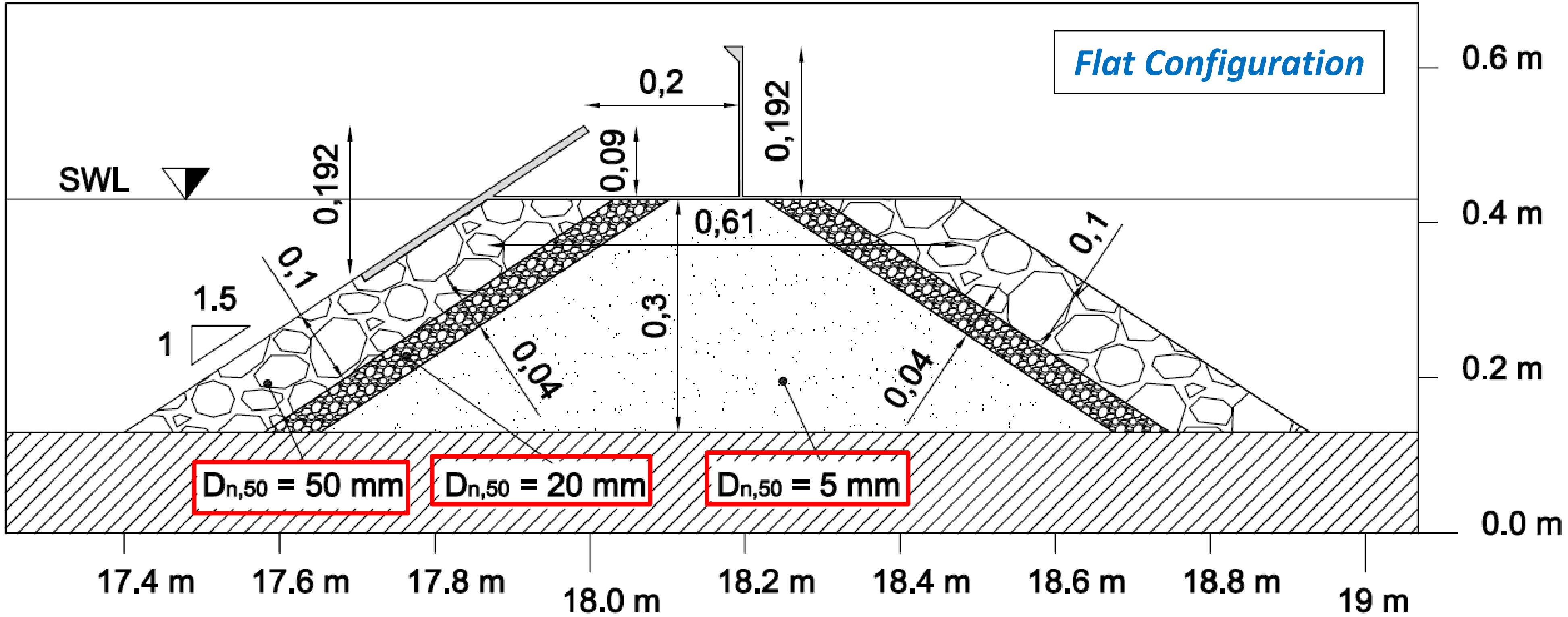

3. DESCRIPTION OF THE EXPERIMENTAL SETUP

28 **pressure transducers**
[14 for each configuration]
[**Fs: 1000 Hz**]

- 5 pt. on the frontal ramp
- 3 pt. on the base
- 5 pt. on the vertical wall
- 1 pt. on the parapet

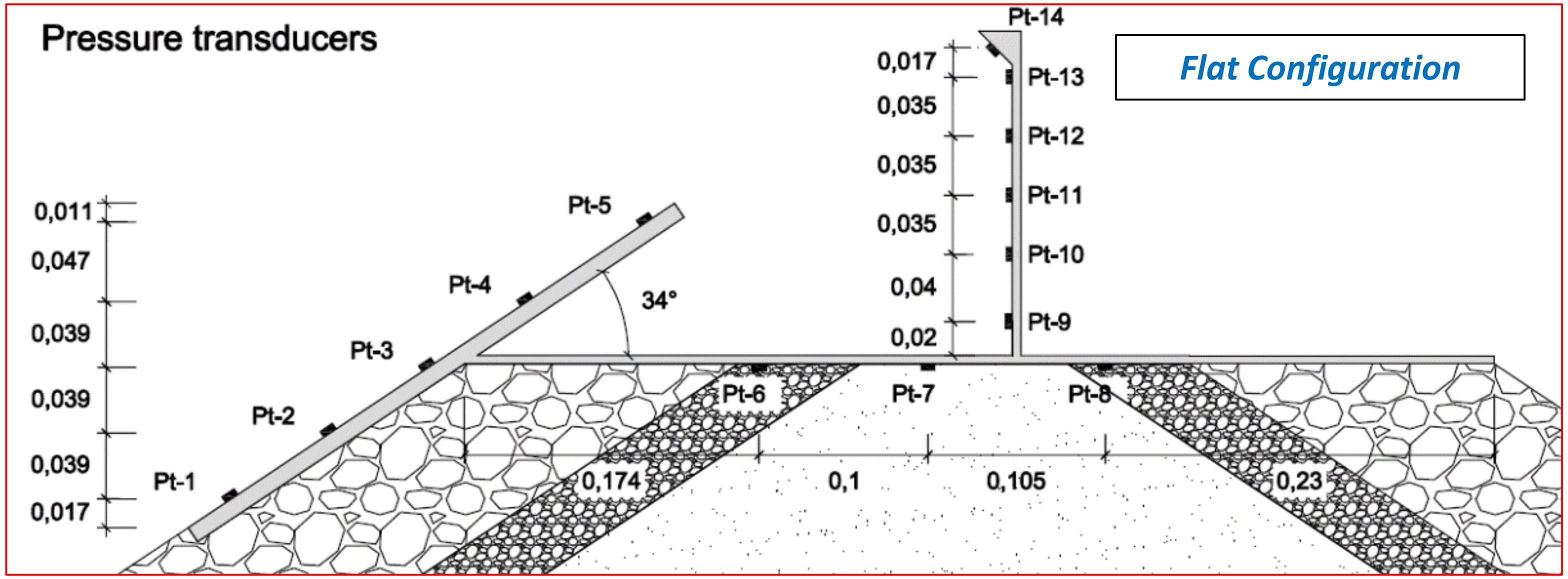

Vertical wall and parapet

Frontal ramp

Base reservoir

OUTLINE

1. INTRODUCTION
2. DESCRIPTION OF THE NUMERICAL MODEL
3. DESCRIPTION OF THE EXPERIMENTAL SETUP
4. NUMERICAL MODEL SETUP
5. RESULTS
6. FUTURE APPLICATIONS
7. CONCLUSIONS

4. NUMERICAL MODEL SETUP

The computational domain is designed to fully replicate the wave flume and the laboratory set-up.

Wave generation

Irregular waves were generated using the **real movement of the wave maker in the laboratory as inputs, X(t) and V(t)**, following the *virtual boundary force method* (*Lara et al., 2011*).

→ **Direct time series comparison** with the signals measured in the laboratory test.

9 tests for the model validation [720 sec]

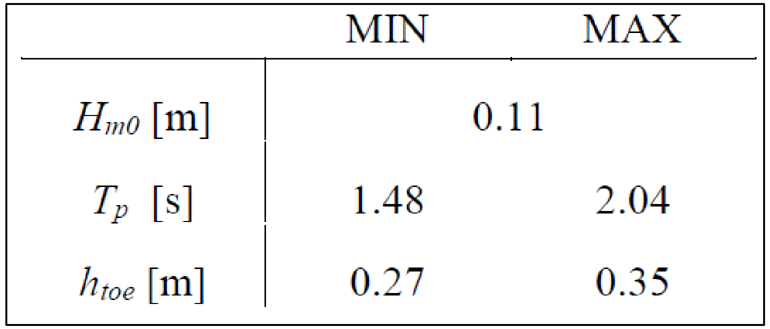

	MIN	MAX
H_{m0} [m]	0.11	
T_p [s]	1.48	2.04
h_{toe} [m]	0.27	0.35

Mesh resolution

- $\Delta y = 5$ mm
- $\Delta x =$ from 30 to 5 mm.

Total of 232,920 cells!!

Selected matching the numerical and experimental results the free surface time series and the pressure at the base reservoir

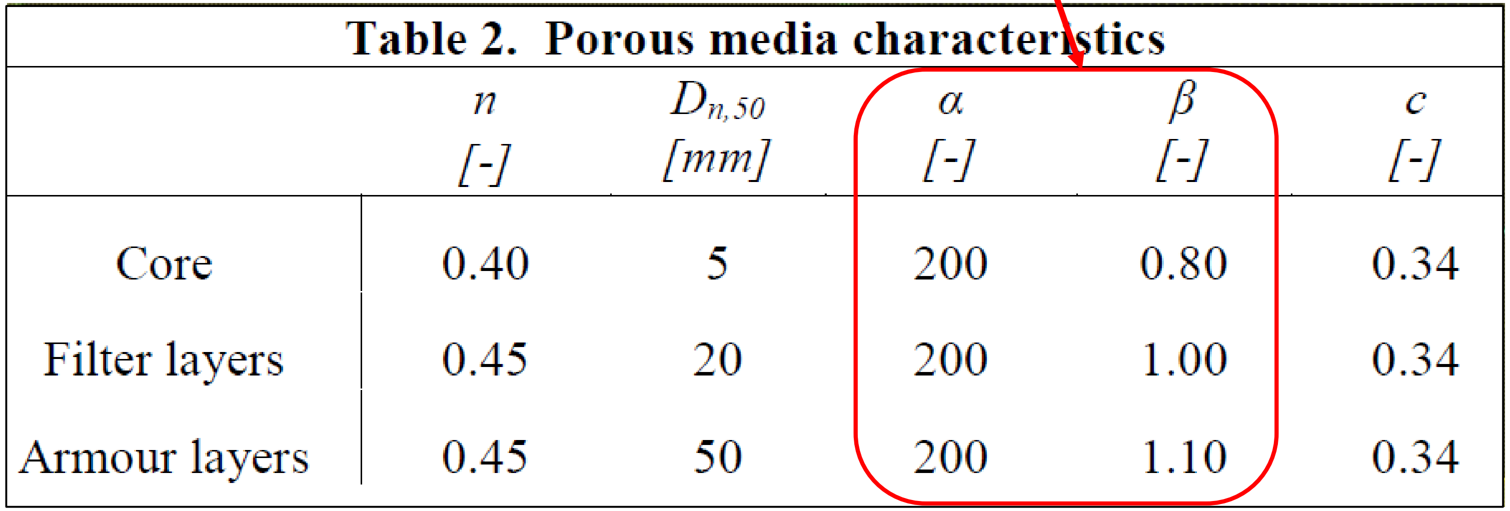

Table 2. Porous media characteristics

	n [-]	$D_{n,50}$ [mm]	α [-]	β [-]	c [-]
Core	0.40	5	200	0.80	0.34
Filter layers	0.45	20	200	1.00	0.34
Armour layers	0.45	50	200	1.10	0.34

OUTLINE

1. INTRODUCTION
2. DESCRIPTION OF THE NUMERICAL MODEL
3. DESCRIPTION OF THE EXPERIMENTAL SETUP
4. NUMERICAL MODEL SETUP
5. RESULTS
6. FUTURE APPLICATIONS
7. CONCLUSIONS

5. RESULTS

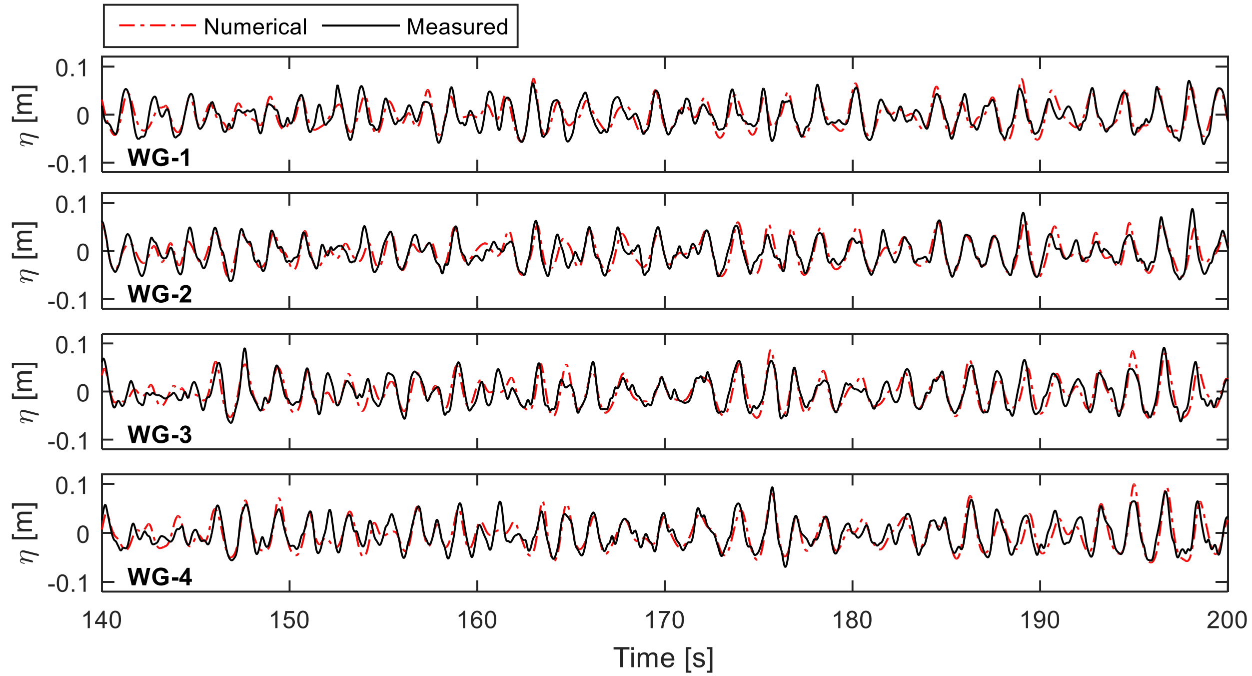

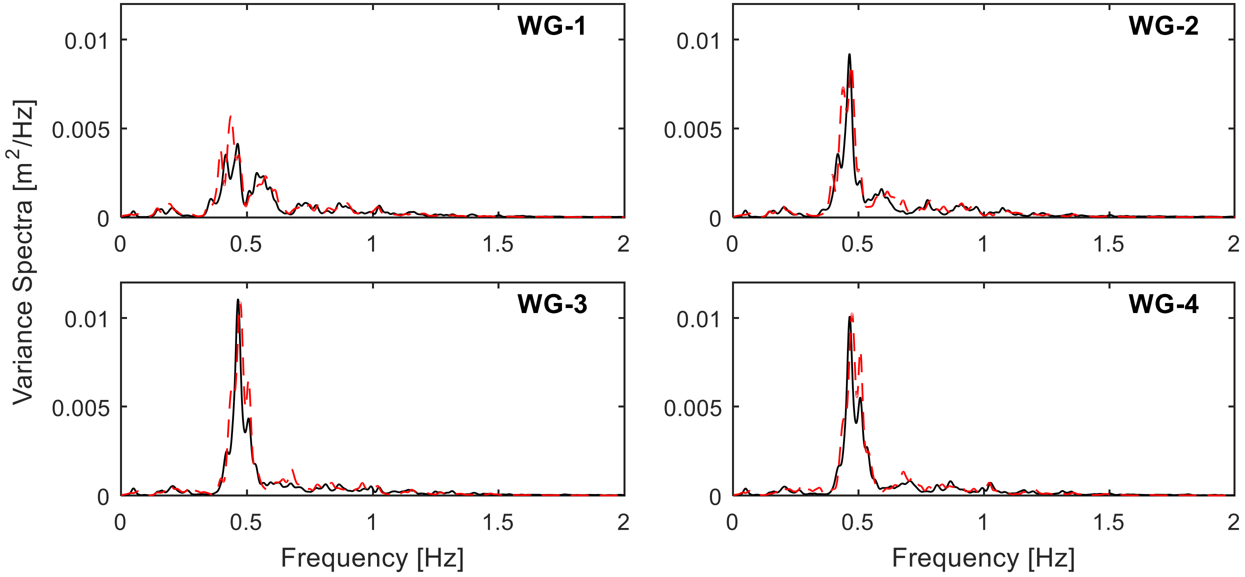

Validation of free surface elevation, wave spectra and wave characteristics

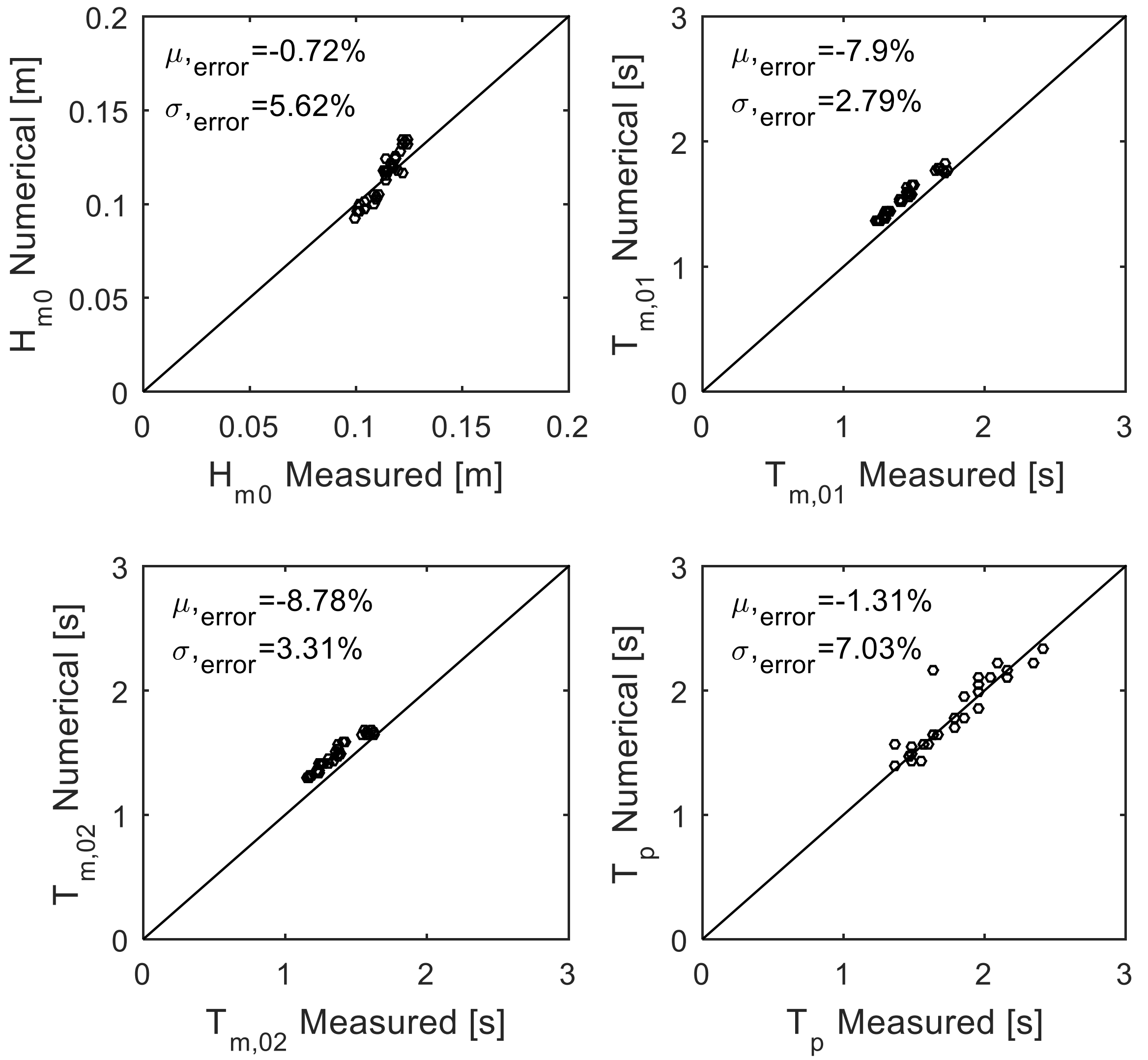

5. RESULTS

Validation of wave pressure

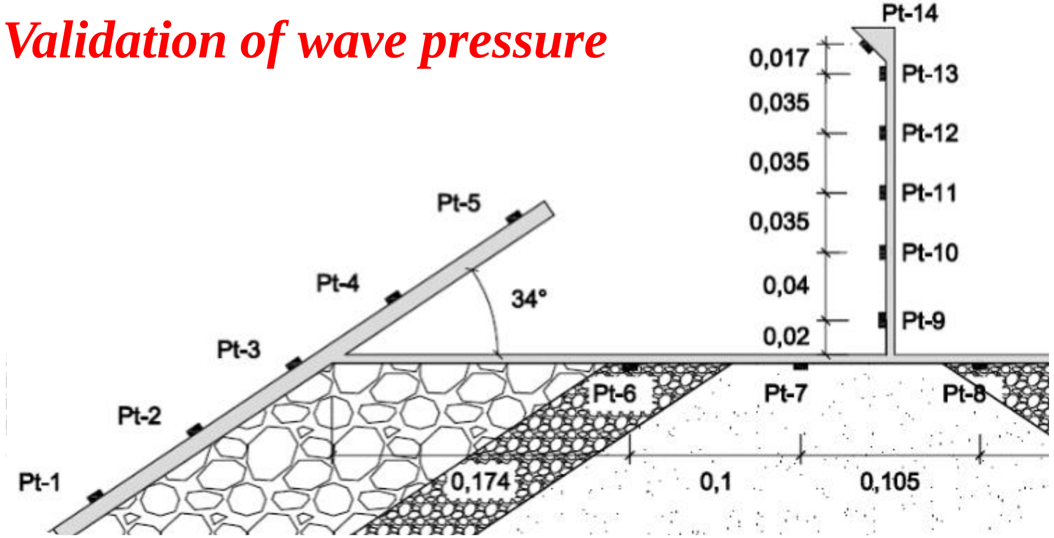

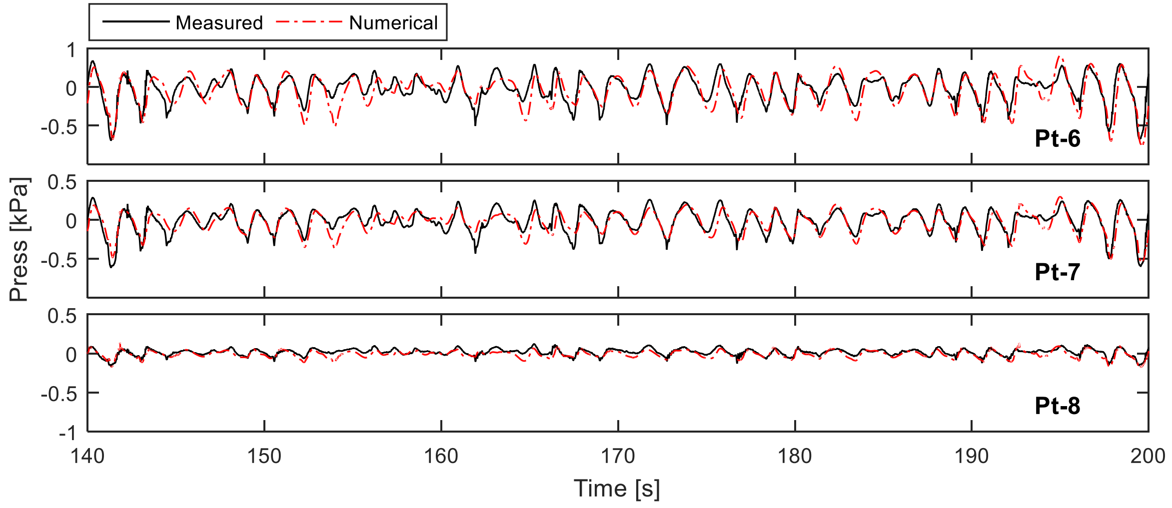

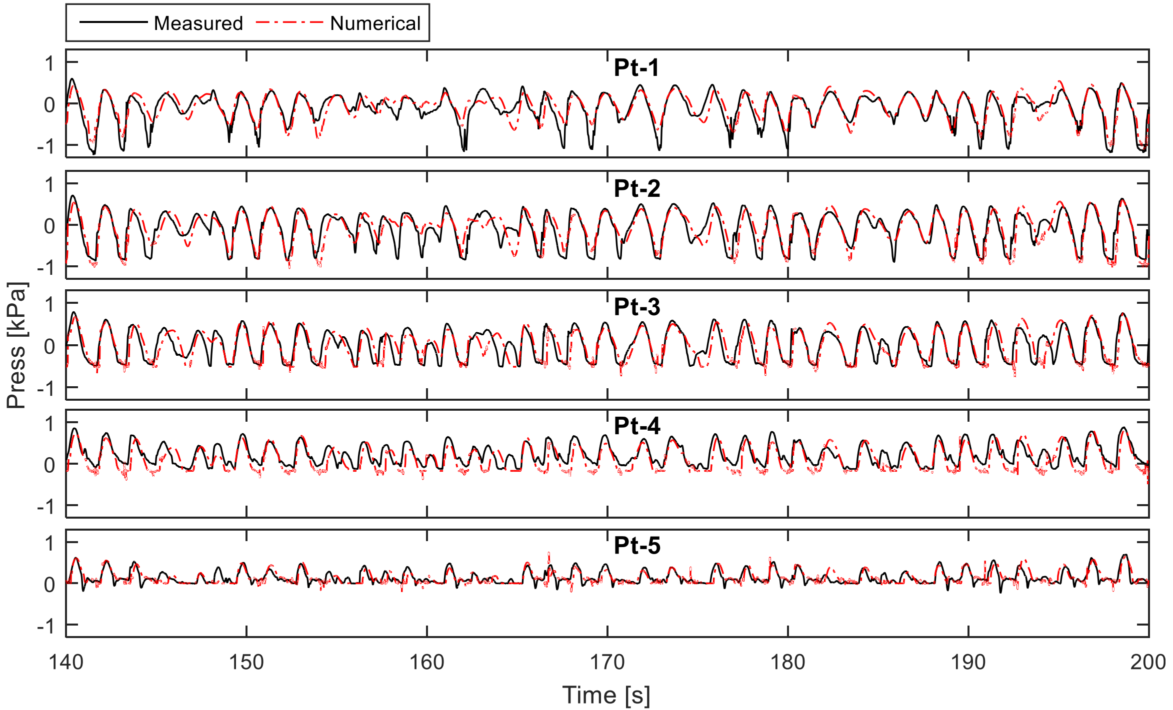

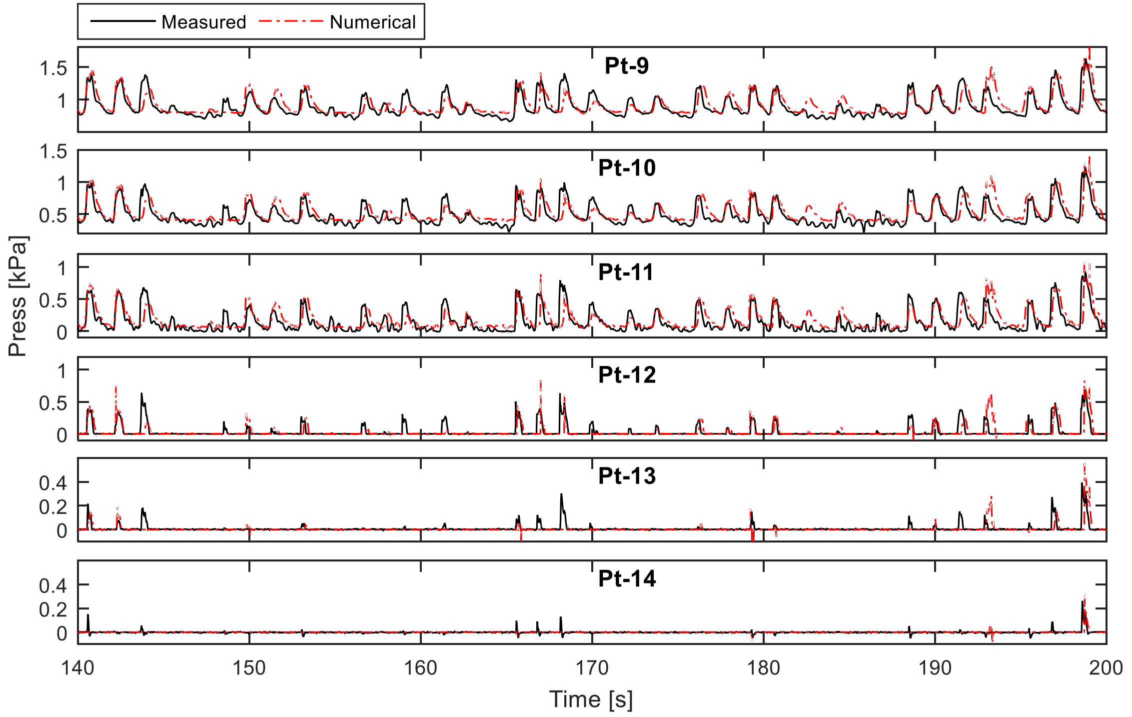

5. RESULTS

Validation of peak pressure

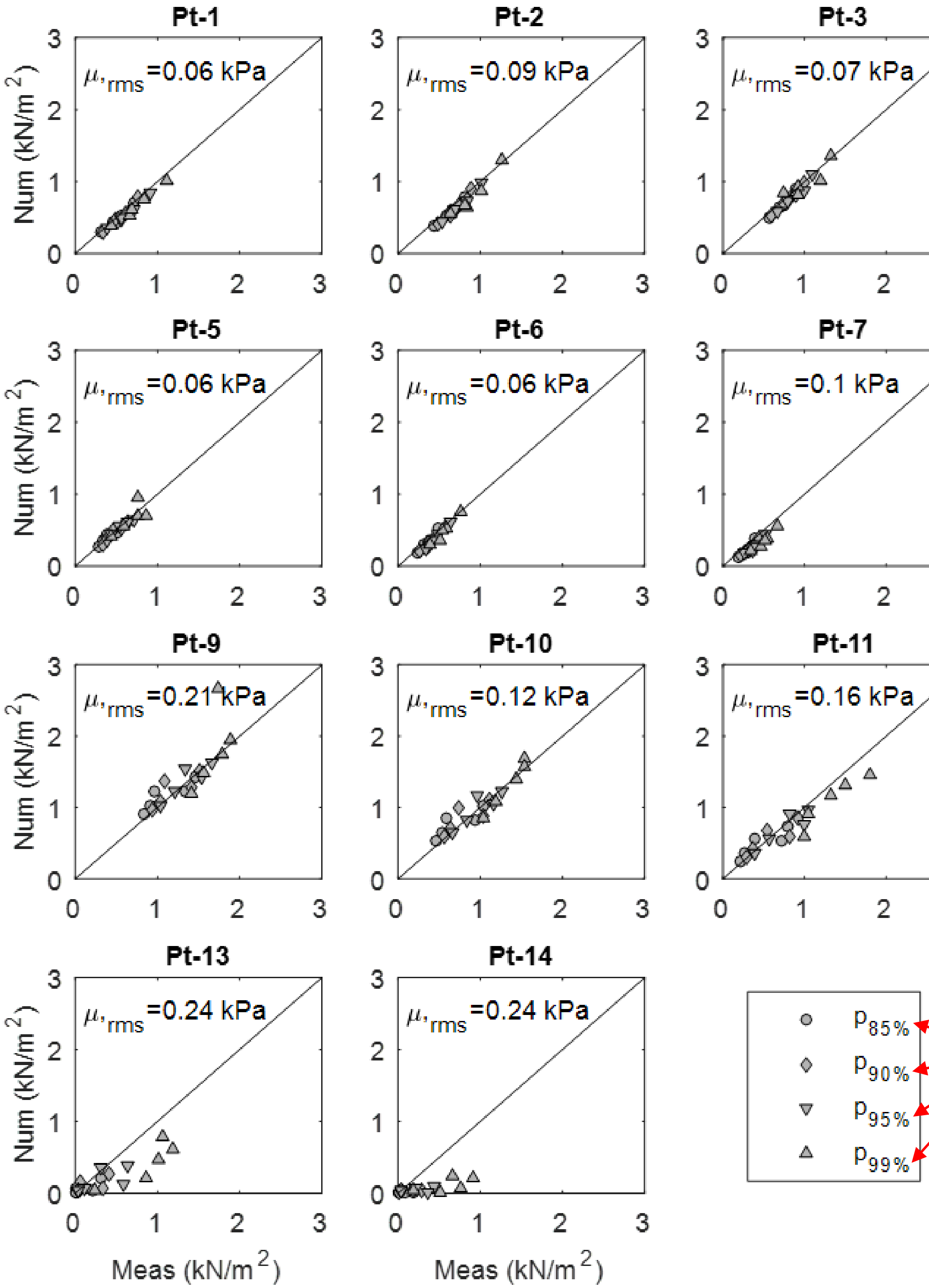

4 percentiles peak pressure

- Very good agreement for wave pressure exerted on the ramp and at the base reservoir.
- Underestimation the pressure acting on the upper part of the vertical wall (Pt-13) and on the parapet (Pt-14)

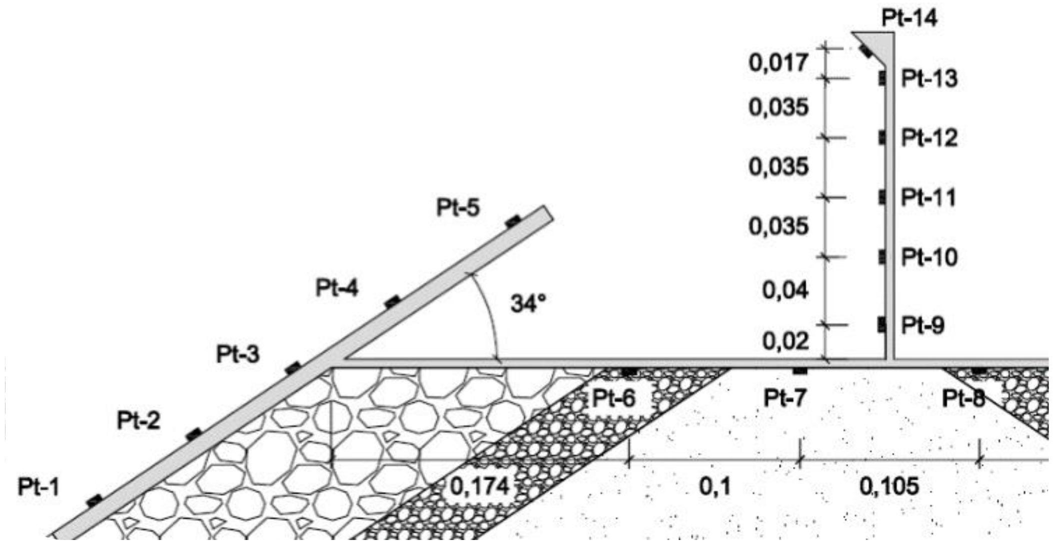

*The measured and numerical data pressure has been **filtered** to avoid noise and unrealistic local peaks.*
*A **digital low-pass filter** is used, with a cut-off frequency of **50 Hz**.*

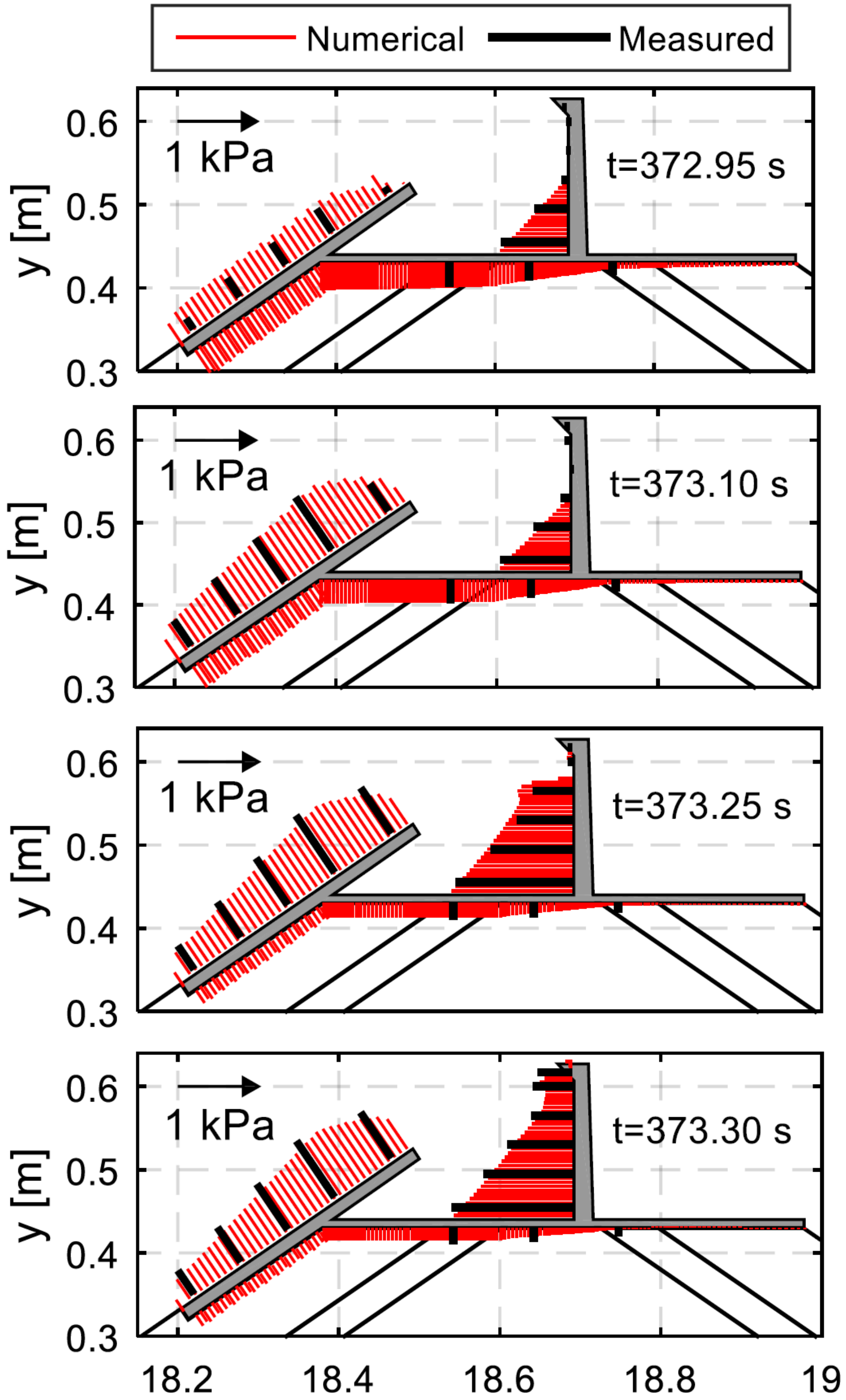

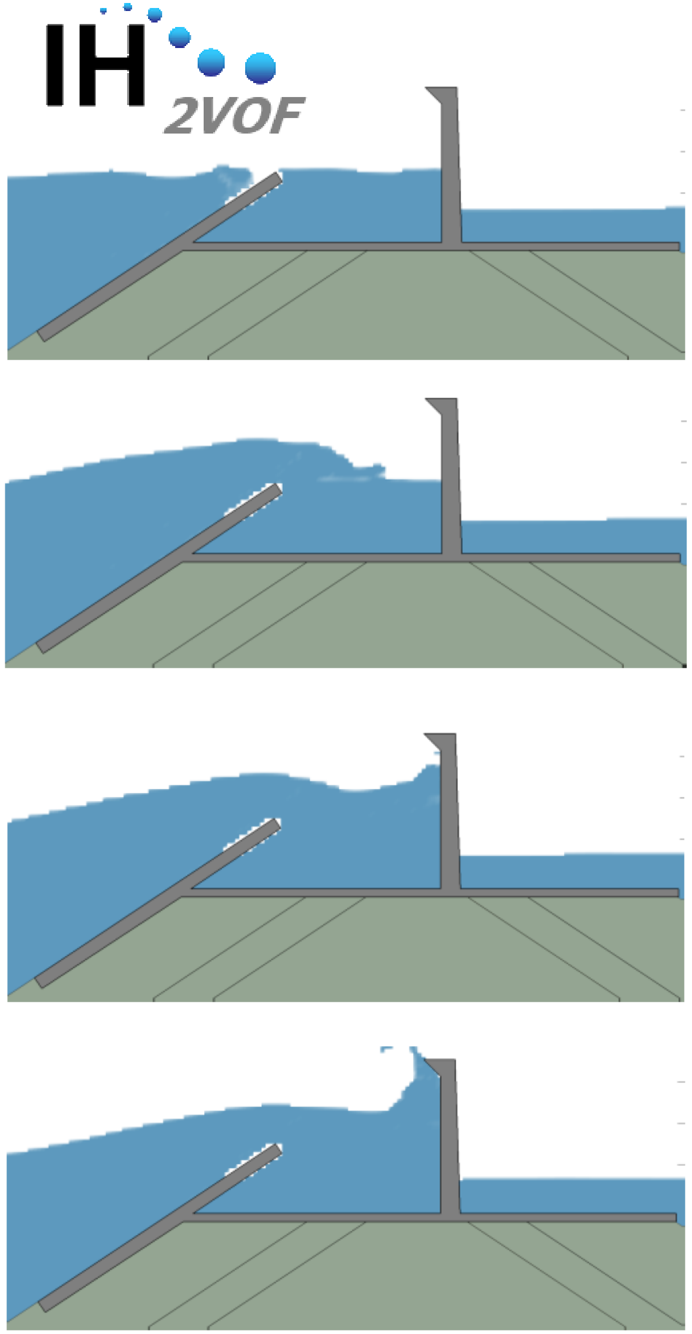

5. RESULTS

Validation of pressure distribuition

The example confirms the model capability of resolving pressure distribution on the OBREC at any time step.

The numerical analysis provides a deeper understanding of the pressure distribution and resultant force in locations where laboratory measurements were difficult to obtain or not available.

In particular, the numerical model provides additional information regarding the pressure distributions underneath the OBREC, where only three transducers were installed during the laboratory tests.

5. RESULTS

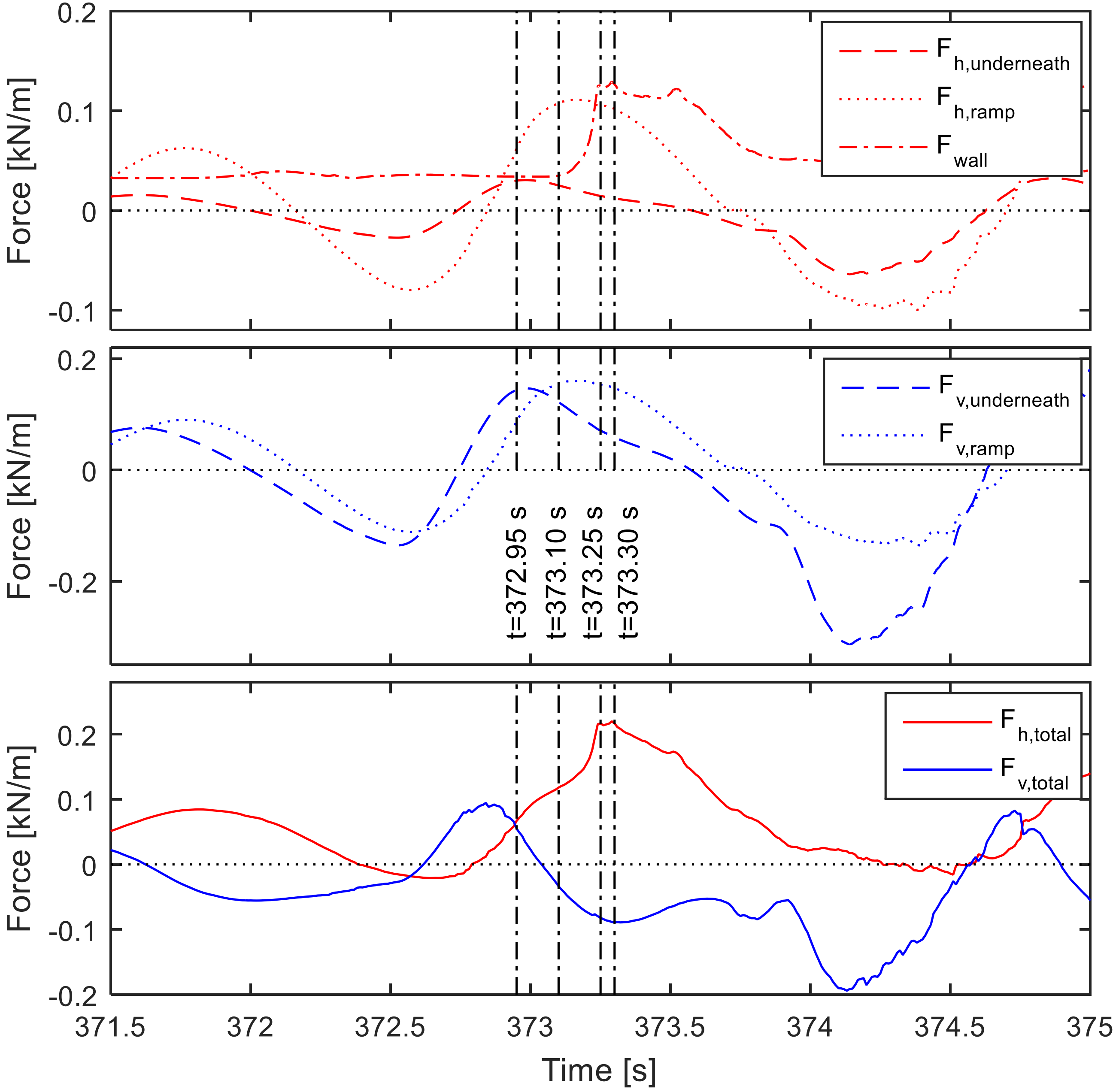

Maximum vertical and horizontal forces are not simultaneous

At the instant of the local maximum total horizontal force, the total vertical force is null or, even more, negative (i.e. overall vertical force directed downward).

At the instant of the local maximum total vertical force, the horizontal force acting on the device is around its minimum value.

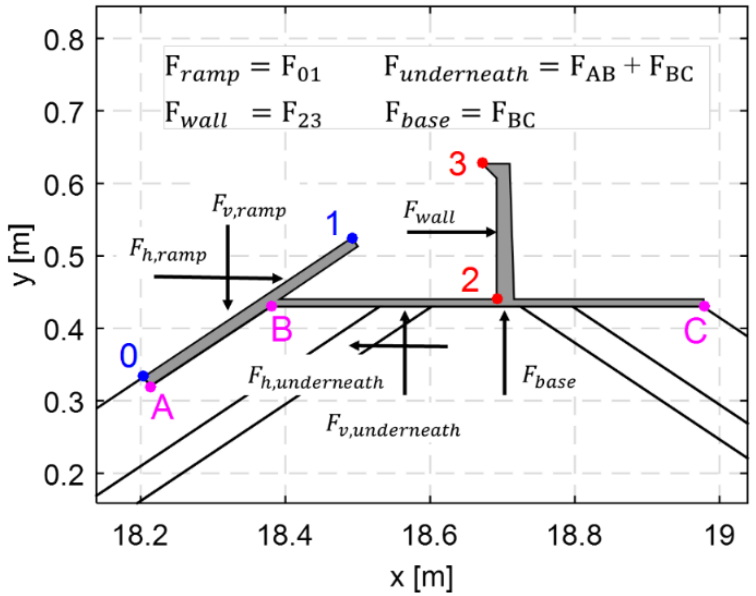

$F_{v,ramp}$, and **$F_{h,underneath}$** improve the global stability of the OBREC, reducing the overall total vertical, **$F_{v,total}$**, and horizontal force, **$F_{h,total}$**, exerted on the device.

5. RESULTS

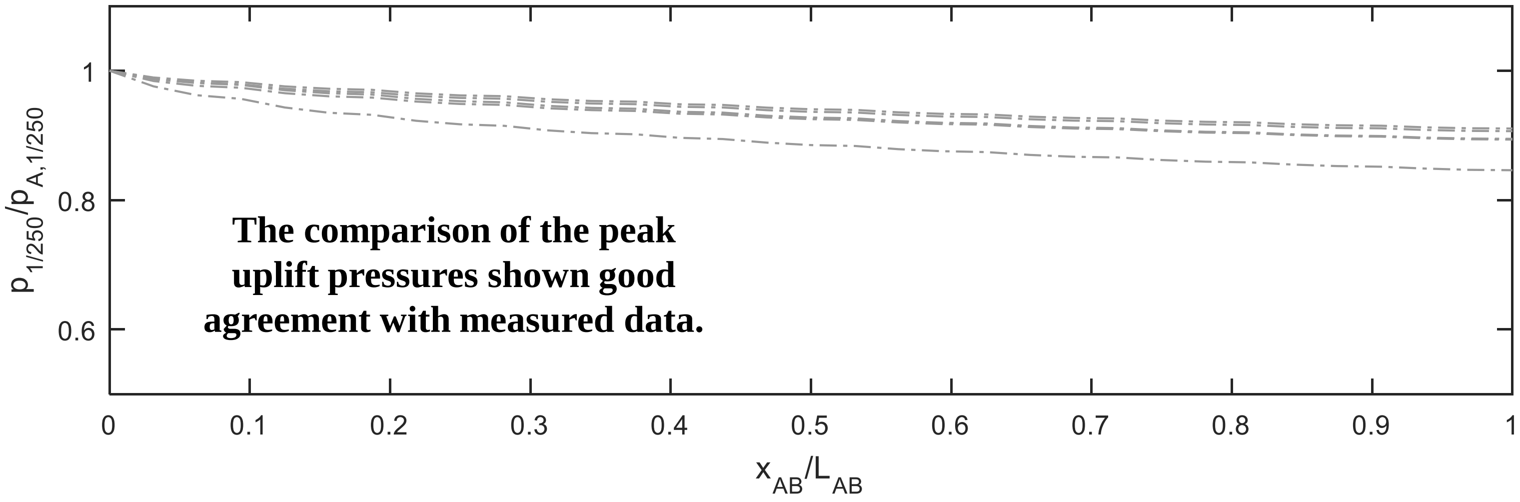

The comparison of the peak uplift pressures shown good agreement with measured data.

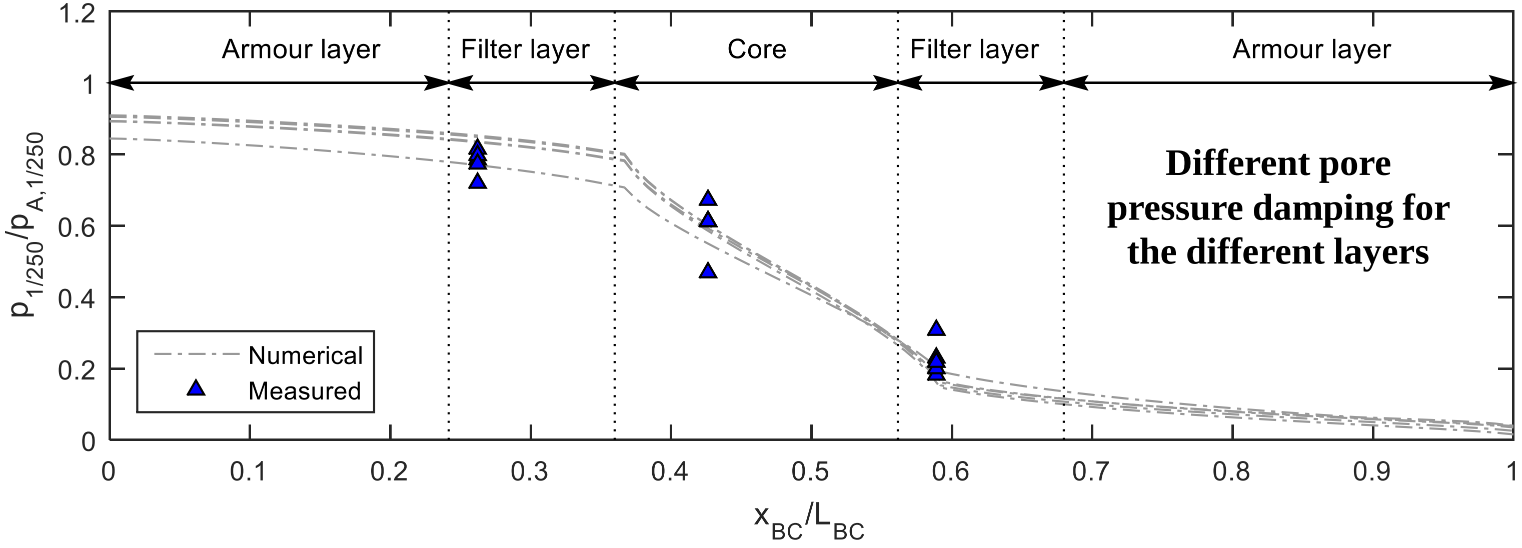

Different pore pressure damping for the different layers

The uplift forces acting on the OBREC calculated numerically can lead to more accurate results

- Uplift forces computed from the measured signal of three pressure transducers are higher than those calculated with the numerical model by integrating the pressure distributions, with a mean error of 17.62%.

- This overestimation is due to the method used to evaluate the forces from the lab data, which is based on linear extrapolation and then it does not take into account the different pore pressure damping produced inside the different layers.

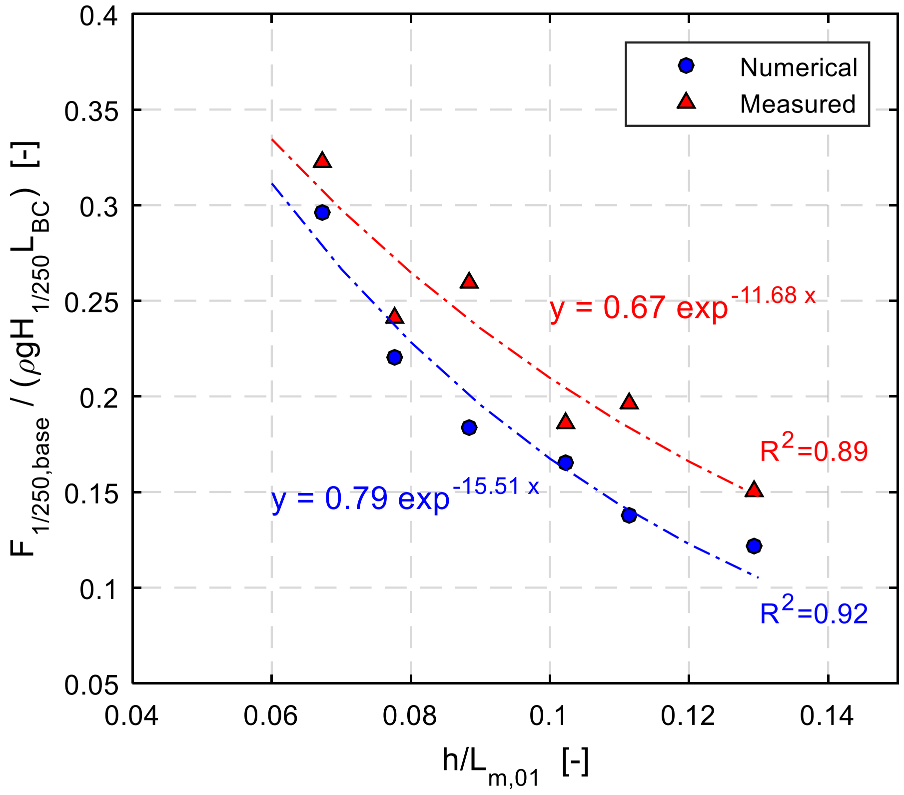

OUTLINE

1. INTRODUCTION
2. DESCRIPTION OF THE NUMERICAL MODEL
3. DESCRIPTION OF THE EXPERIMENTAL SETUP
4. NUMERICAL MODEL SETUP
5. RESULTS
6. FUTURE APPLICATIONS
7. CONCLUSIONS

6. FUTURE APPLICATIONS

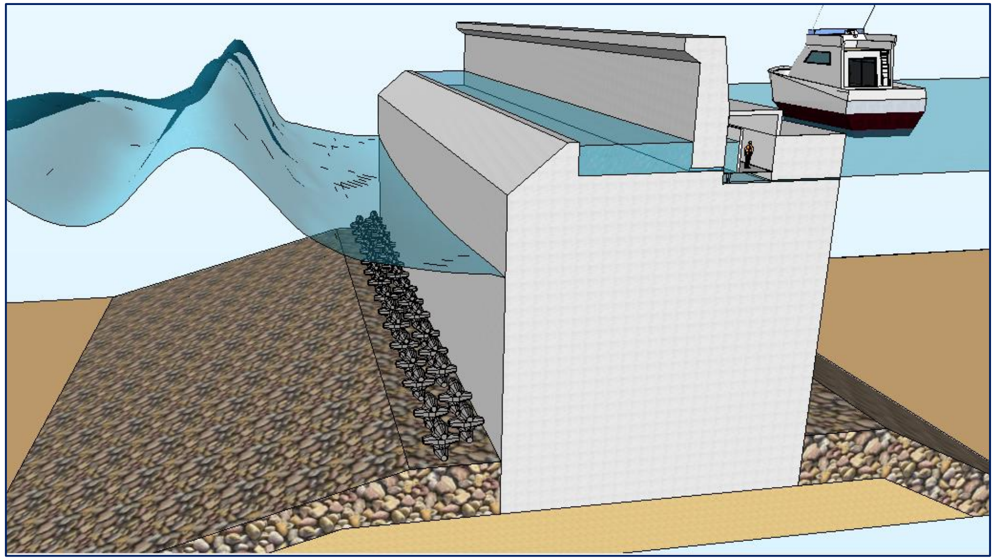

Further numerical analyses are carried out to study the stability analysis and hydraulic performances of **innovative devices** integrated into **vertical caissons.**

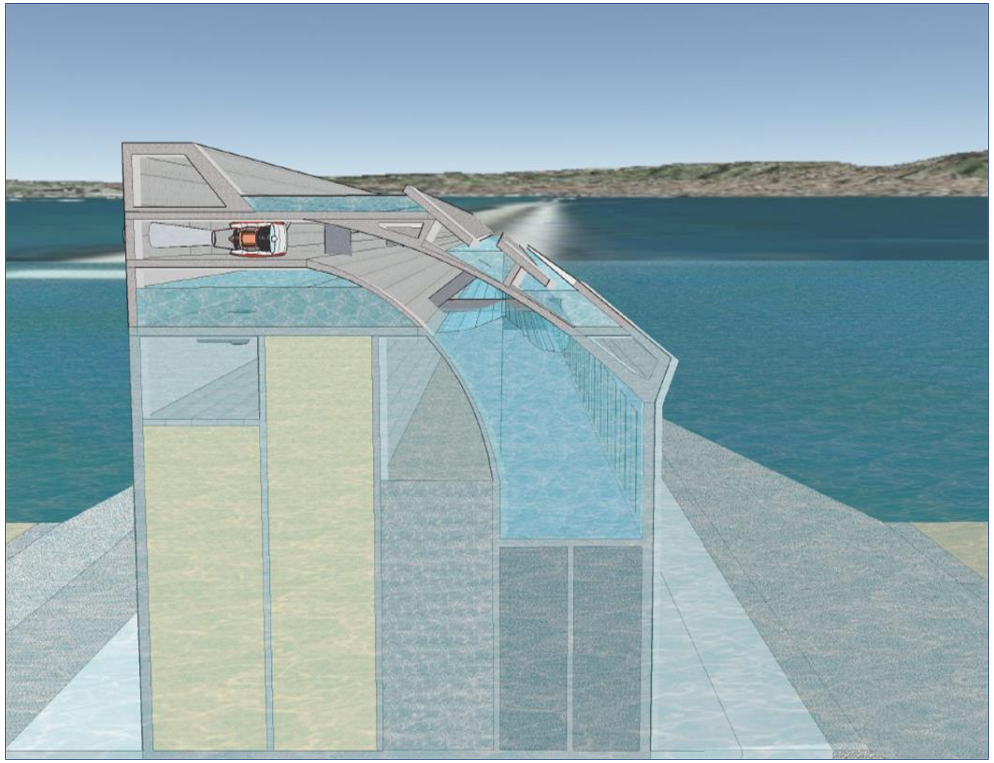

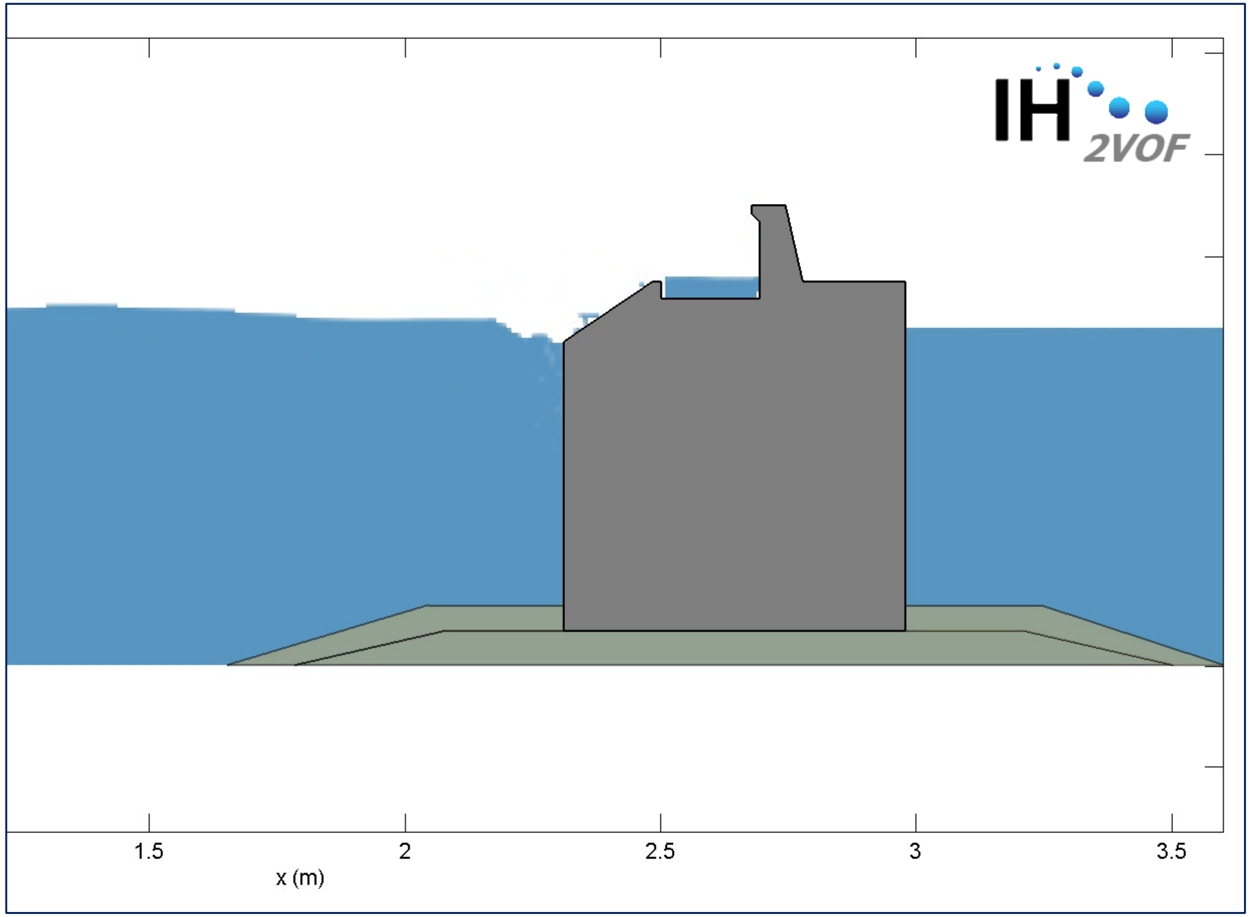

6. FUTURE APPLICATIONS

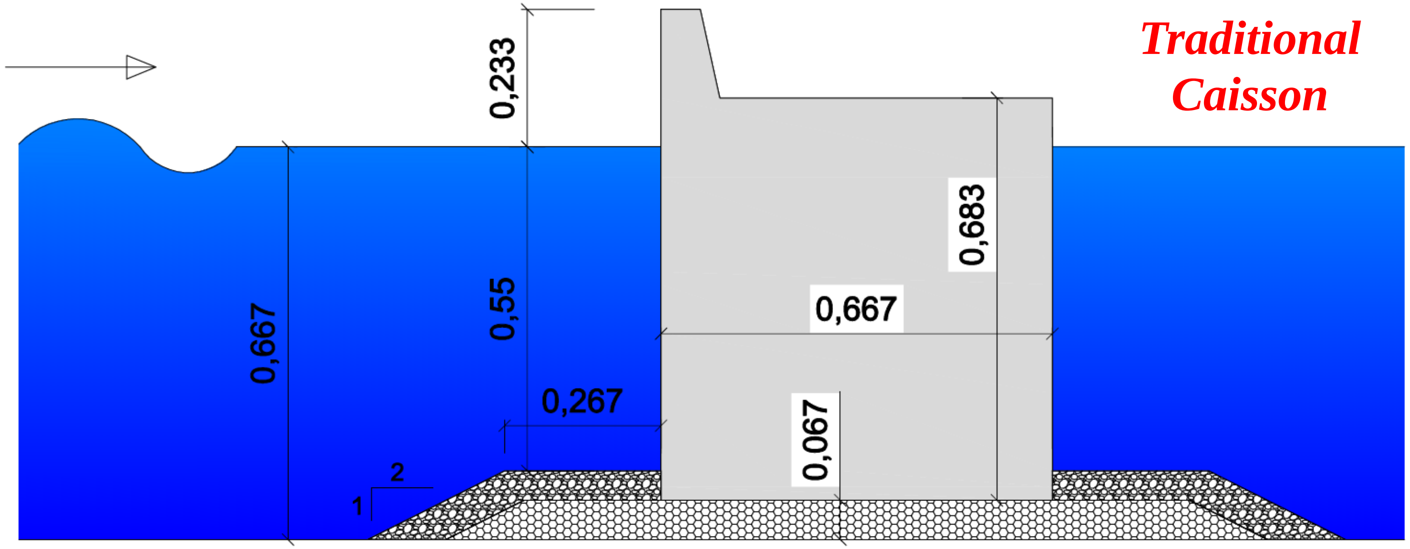

Traditional Caisson

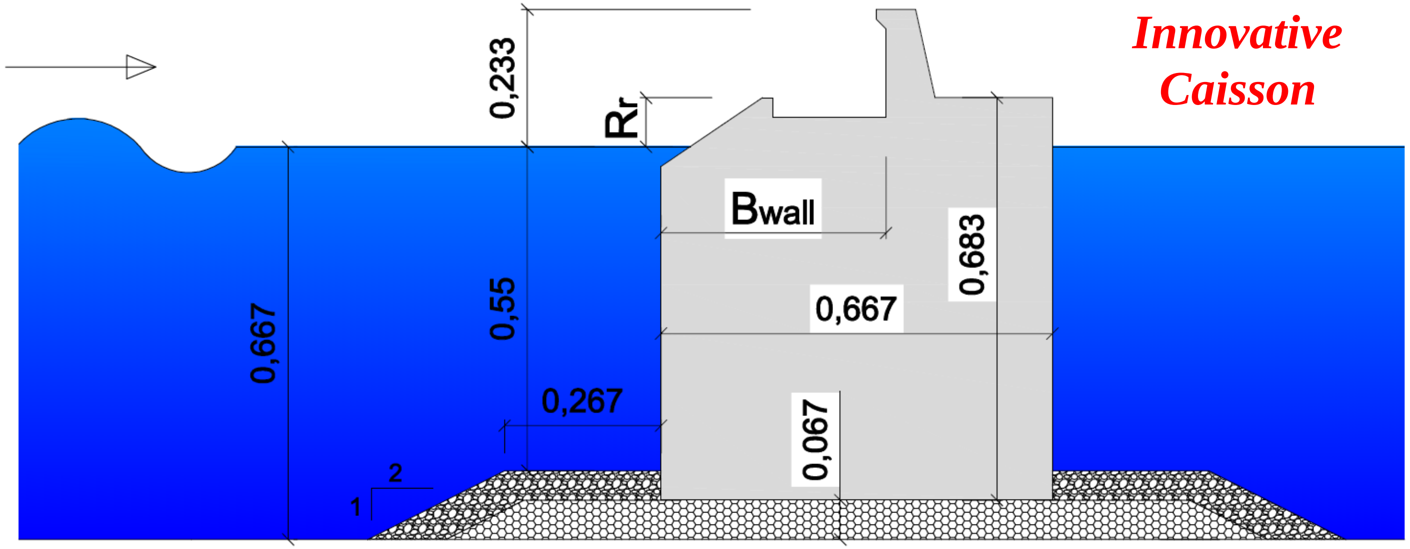

Innovative Caisson

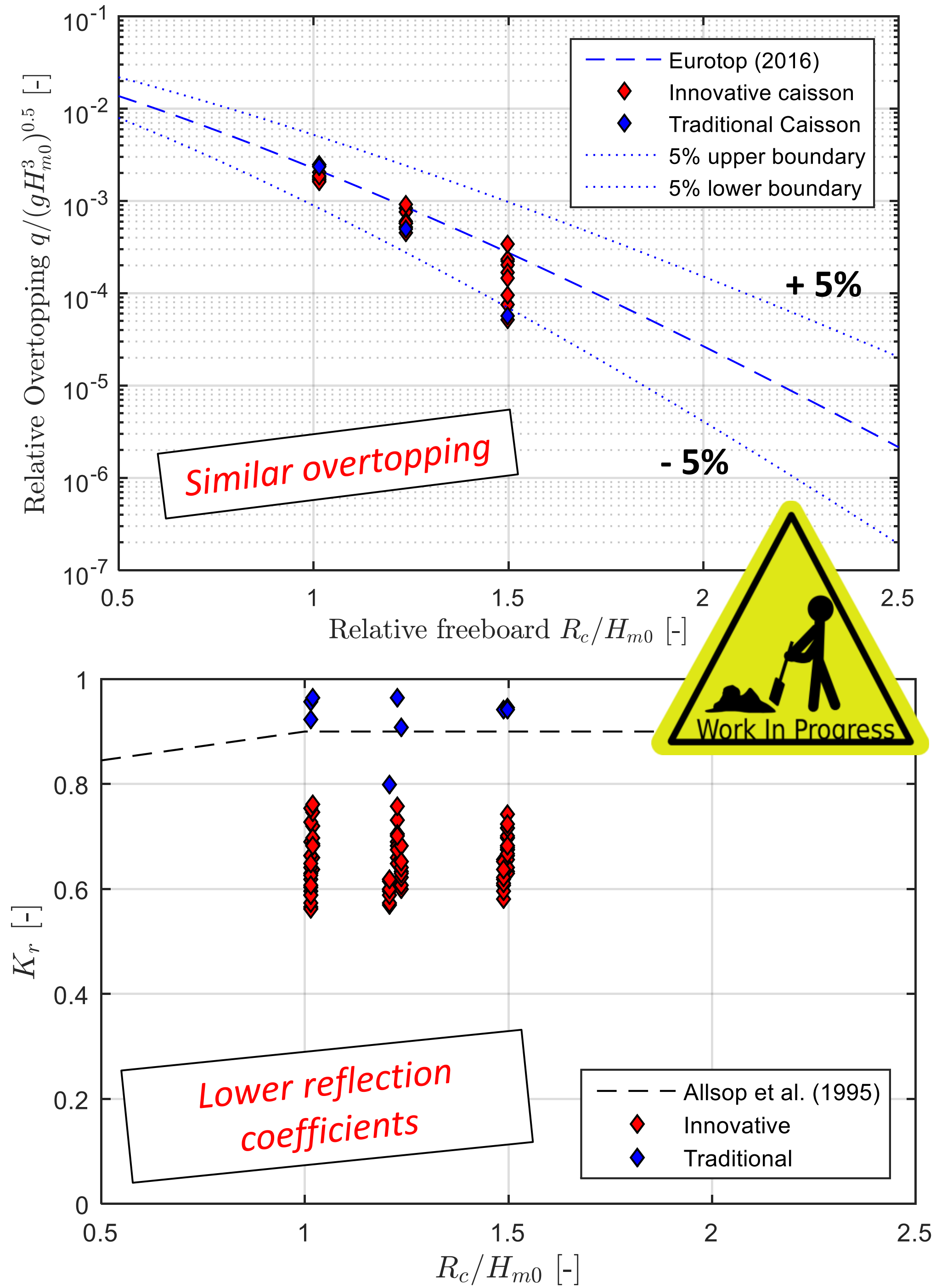

Similar overtopping

Lower reflection coefficients

OUTLINE

1. INTRODUCTION
2. DESCRIPTION OF THE NUMERICAL MODEL
3. DESCRIPTION OF THE EXPERIMENTAL SETUP
4. NUMERICAL MODEL SETUP
5. RESULTS
6. FUTURE APPLICATIONS
7. CONCLUSIONS

6. CONCLUSIONS

- The **wave – structure interaction** of the OBREC has been investigated using **IH-2VOF** model.
- The **validation** against physical model test is based on the comparison of the free surface elevation in front of the structure and the wave loading acting on the device.
- Numerical model very well simulates the interaction of the waves with the structure.
- The obtained **wave pressure** are highly satisfactory when compared with measured data.
- The numerical analysis is used to extend the results of the physical model test campaign, providing a deeper understanding of the loading in locations where laboratory measurements were not available.

IH-2VOF can be used as a **complementary tool** in the design process
of non-conventional breakwater with complex geometries, such as the OBREC device.

Thank you for your attention